Biol. Cybern. 74, 275–286 (1996)

Biological Cybernetics

A columnar model of somatosensory reorganizational plasticity based on Hebbian and non-Hebbian learning rules

F. Joublin, F. Spengler, S. Wacquant, H.R. Dinse

Institut für Neuroinformatik, Lehrstuhl für Theoretische Biologie, Ruhr-Universität Bochum, D-44780 Bochum, Germany
(e-mail: joublin@neuroinformatik.ruhr-uni-bochum.de)

Received: 24 July 1995 / Accepted in revised form: 26 October 1995

Abstract. Topographical and functional aspects of neuronal plasticity were studied in the primary somatosensory cortex of adult rats in acute electrophysiological experiments. Under these experimental conditions, we observed short-term reversible reorganization induced by intracortical microstimulation or by an associative pairing of peripheral tactile stimulation. Both types of stimulation generate large-scale and reversible changes of the representational topography and of single cell functional properties. We present a model to simulate the spatial and functional reorganizational aspects of this type of short-term and reversible plasticity. The columnar structure of the network architecture is described and discussed from a biological point of view. The simulated architecture contains three main levels of information processing. The first one is a sensor array corresponding to the sensory surface of the hind paw. The second level, a pre-cortical relay cell array, represents the thalamo-cortical projection with different levels of excitatory and inhibitory relay cells and inhibitory nuclei. The array of cortical columns, the third level, represents stellate, double bouquet, basket and pyramidal cell interactions. The dynamics of the network are ruled by two integro-differential equations of the lateral-inhibition type. In order to implement neuronal plasticity, synaptic weight parameters in those equations are variables. The learning rules are motivated by the original concept of Hebb, but include a combination of both Hebbian and non-Hebbian rules, which modifies different intra- and inter-columnar interactions. We discuss the implications of neuronal plasticity from a behavioral point of view in terms of information processing and computational resources.

1 Introduction

1.1 Survey of post-ontogenetic plasticity

Neural systems organize behavior according to the environmental conditions. However, the environment and the constraints it imposes changes on a variety of time scales. Therefore, each system operating in such an environment must preserve considerable life-long adaptive capacities beyond the critical developmental period, for which we introduced the term "post-ontogenetic plasticity" (Dinse et al. 1993; Spengler and Dinse 1994).

In recent years, post-ontogenetic plasticity has been observed in the cortex of many adult species: after circumscribed damage to peripheral receptor arrays of the skin, cochlea or retina, the input-deprived cortical areas are occupied by the representations of neighboring sensory fields after weeks and months of recovery (Merzenich et al. 1984; Pons et al. 1988; Robertson and Irvine 1989; Kaas et al. 1990; Gilbert and Wiesel 1992; Eysel 1992; Garraghty and Kaas 1992). Parallel to lesion-related and injury-related reorganization, evidence has accumulated that primary sensory representations are similarly remodeled following behavioral training, classical conditioning or prolonged natural sensory stimulation, indicating that cortical maps and receptive fields are also subject to modification by use (Weinberger et al. 1990; Scheich 1991; Recanzone et al. 1992b, c, 1993; Pascual-Leone and Torres 1993; Xerri et al. 1994; Godde et al. 1994; Spengler et al. 1995). The impact of these findings extends plastic reorganizational processes to the field of higher cognitive functions related to learning and implicit memory functions. Input-related cortical plasticity may therefore represent the neural basis of life-long adaptive sensory and perceptual capacities. The time constants of these phenomena range from a few seconds to several months and years. Accordingly, a multiplicity of different mechanisms can be assumed to account for different types of cortical plasticity. The short time scale of many reorganizational processes related to use-dependent plasticity and their reversibility support the hypothesis of fast modulations of synaptic efficiency in neuronal networks that do not necessarily involve anatomical changes (Garraghty and Kaas 1992; Antonini and Stryker 1993; Darian-Smith and Gilbert 1994). It has been stated that many of the changes are not attributable to so-called strictly Hebbian rules (Merzenich and Sameshima 1993).

Our specific interest concentrates on fast and reversible plastic reorganizational processes. We and others have demonstrated that a few hours of intracortical microstimulation (ICMS), which utilizes repetitive electrical pulse trains

Correspondence to: F. Joublin

delivered via a microelectrode, induce short-term plasticity (Dinse et al. 1990, 1993; Nudo et al. 1990; Sirois and Hand 1991; Recanzone et al. 1992a; Bedenbaugh et al. 1992; Spengler and Dinse 1994). To extend the experimental paradigm to a more natural type of stimulation, we introduced an associative pairing protocol of simultaneously applied tactile stimulation (pairing of peripheral tactile stimulation, PPTS). A few hours of PPTS result in reorganizational changes comparable to those reported for ICMS and are similarly effective in the induction of fast plasticity at a perceptual level in humans (Godde et al. 1994; Dinse et al. 1995). The basic methodological approaches and the main results of the ICMS and PPTS experiments are summarized in Sect. 2 and described in more detail elsewhere (Dinse et al. 1993, 1995; Spengler and Dinse 1994).

1.2 Simulations

In general, designing a model of neuronal plasticity has to address the question of an appropriate level of description, such as the level of physiological mechanisms at synaptic locations, including single channel modulation and molecular transfer, the level of single cells, or the level of entire neuronal networks and representational maps. Neuronal plasticity in the somatosensory system has already been modeled at the network level to understand long-term reorganization resulting from amputations or lesions (Pearson et al. 1987; Grajski and Merzenich 1990; Ritter et al. 1990), whereas others (Andres et al. 1994) have dealt in a more abstract way with aspects of short-term plasticity using a feature map approach. The goal of our simulation is to study the short-term dynamical behavior of cell populations during fast reorganization at the level of representational maps and networks.

Assuming that structural aspects of the architecture of the brain are closely related to its functional properties, we have simulated a cortical area with a columnar structure, which shares some common properties with previous columnar models (Burnod 1988; Favorov and Kelly 1994). This basic columnar organization allows us to distinguish between short-range intra-columnar and long-range inter-columnar plasticity to explain both topographical and functional reorganization. In this framework, we can analyze the possible roles of the underlying learning rules operating within the network structure.

In Sect. 3, we describe and discuss the physiological relevance of the main hypothesis required to build the model and present results of the simulations. In Sect. 4, we discuss some possible mechanisms involved in the generation of the observed plastic changes and provide an explanation for the differential effects found after ICMS and PPTS.

2 Biological experiments

2.1 Experimental protocols

The electrophysiological experiments were performed in primary somatosensory cortex of urethane anesthetized adult rats. Treatment of all animals was within the US NIH Principles of Laboratory Animal Care (revised 1987). For details of experimental procedures see Spengler and Dinse (1994) and Dinse et al. (1995). Neuronal activity of single units, or of small clusters of neurons, was recorded extracellularly at depths of 600–800 μm (layer IV) using glass microelectrodes filled with 3 M NaCl. Penetrations were usually placed 100–200 μm apart, which allowed us to define the spatial extent and topography of the hind paw representation and its borders.

ICMS was delivered with 13 pulses of 6 μA, 0.2–1 ms duration, in 40-ms trains delivered at 1 Hz at a so-called microstimulation site (ss), whose corresponding receptive field[1] (RF) is denoted as ssRF. The other penetration sites were called recording sites (rs) and had corresponding RFs denoted rsRFs (Fig. 1). To induce plastic changes by PPTS, the centers of two non-overlapping RFs were simultaneously stimulated for several hours according to the following protocol: a train of eight different interstimulus intervals between 100 and 3000 ms was used randomly followed by a pause of 15 s. To demonstrate that the PPTS effects were in fact due to the associative pairing, we used an additional protocol, in which only one selected skin location (single point peripheral stimulation, SPPS) was stimulated using the same stimulation parameters as in the PPTS protocol. As a rule, the hind paw representation was mapped[2] in detail, defining cutaneous low-threshold RFs before and after the experimental manipulation (pre- and post-ICMS, pre- and post-PPTS).

Functional aspects of cortical reorganization were studied by analyzing the transfer properties of neurons before and after ICMS by variation of the frequency of tactile stimulation (interstimulus interval, ISI) and of stimulus amplitude. A mechanical stimulator was used to apply computer-controlled tactile stimuli of 8 ms duration at 1 Hz or at various ISIs at the RF centers either at the recording site or at the microstimulation site. For quantitative analysis, post-stimulus-time histograms (PSTHs) were compiled. Neuronal responses were analyzed for peak response latency (time between stimulus onset and time of maximal response) and response peak (number of spikes during response peak). Tuning curves were constructed by plotting neural responses as a function of ISI or stimulus amplitude.

2.2 Experimental results

Under control conditions, the rat SI hind paw representation is characterized by small, low-threshold, cutaneous RFs. Within a fine-grained and highly ordered topography, single digits are located rostral to the pads and the more distally located RFs represent parts of the heel.

2.2.1 Topographic aspects of cortical reorganization induced by ICMS. Application of 2–4 h of ICMS in the center of the hind paw representation caused an overall expansion of the stimulated skin representation (Fig. 2, left). The ssRF was

[1] RFs in biological experiments are always related to the sensory surface. In simulations, however, RFs are usually defined as the "dendritic arborization" or the set of connections arriving at their formal neurons.

[2] We use the term "mapping" to describe the process of tactile stimulation of the hind paw to determine the RF of each penetration site.

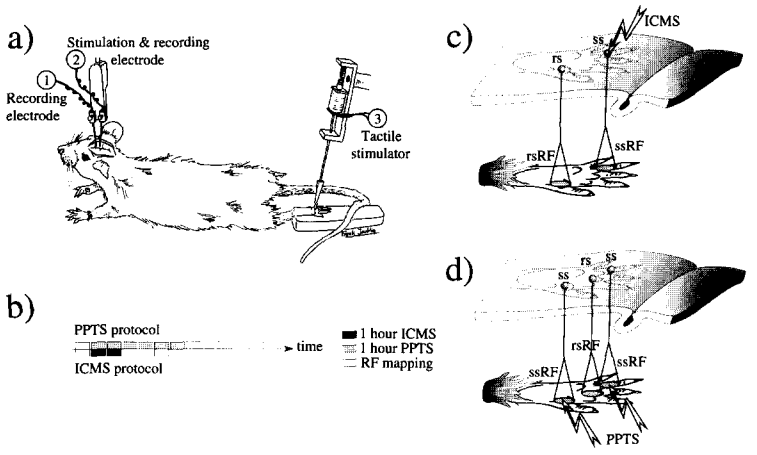

Fig. 1a–d. Experimental setups. **a** Electrophysiological recordings in the primary somatosensory cortex (SI) and stimulation devices. To induce cortical reorganization for ICMS experiments, one of the recording sites (1) was defined as the stimulation site and the other (2) as the recording site; tactile stimulation was applied by a mechanical stimulator (3). In PPTS/SPPS experiments, only one electrode was used to record in SI (1) and one (SPPS) or two (PPTS) tactile stimulators (3) were used during the experiment. **b** Time scale for ICMS and PPTS protocols and receptive field (RF) mapping procedures, before and after experimental manipulation. **c**, **d** Schematic drawings of cortical penetration sites (rs, recording site; ss, stimulation site) and cutaneous receptive fields (*rsRF*, *ssRF*: for details see text) in an ICMS experiment (**c**) and in a PPTS experiment (**d**)

increased, and similarly increased skin fields were found at recording sites (rsRFs) close to the microstimulation site, revealing a distance-dependent, directed enlargement towards the control ssRF. The mean RF size increased several-fold after ICMS. Thus, the fine-grained topography of the hind paw was replaced by a coarse representation dominated by the representation of the ssRF.

A few hours of ICMS at the rostral border of the hind paw representation generated reorganizational changes across functionally defined areal borders of SI and motor cortex. Newly induced skin field representations contained selective skin representations of the ICMS site in previously non-somatic cortical regions, from where low-threshold movements could be elicited. In this way, individually defined areal borders could be reversibly relocated over distances up to 800 μm. Generally, early ICMS-related effects could be detected after 15 min, and much greater effects were visible after 2–3 h of ICMS. The changes were fully reversible within 6–8 h after terminating ICMS (Spengler and Dinse 1994).

2.2.2 Functional aspects of cortical reorganization induced by ICMS. The neuronal transfer characteristics (tuning curves) obtained for variation of ISIs and for variation of stimulus amplitudes can be described as low-pass filters. Statistical analysis was used to compare correlations between ss-cell and rs-cell responses before and after ICMS. Functional adaptation was defined between cell responses which had been uncorrelated pre-ICMS and became correlated post-ICMS (correlation factor $r \geq 0.8$) (Fig. 3a). Functional loss of selectivity was defined as a 50% decrease of the standard deviation within the response across the applied stimulus variation (i.e., ISI; Fig. 3b).

We found that cells were differentially affected by ICMS. The rs-cells adopted the ss-cells' tuning after ICMS, thus changing their tuning properties. In contrast, the ss-cells lost their selectivity due to a general broadening and flattening of their tuning.

Response latencies at rs to tactile ssRF stimulation were normally delayed by 4–6 ms. After ICMS, the latencies were shortened and came to match those measured at the rsRF. Pre- and post-ICMS firing rates were about the same for ss and rs, but recording sites stimulated at the ssRFs before ICMS showed on average 70% lower firing rates. After ICMS these differences disappeared, indicating similar effectiveness of tactile stimulation at the two recording sites (Spengler 1993).

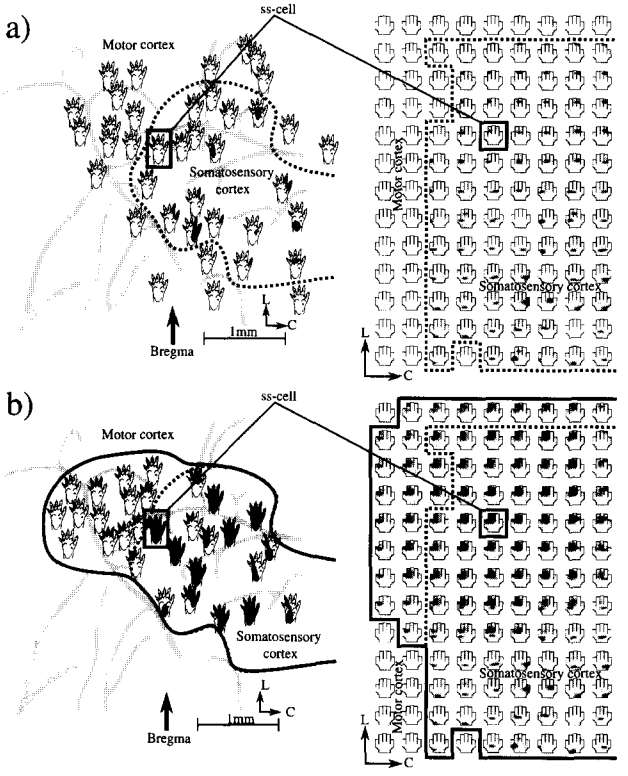

Fig. 2. Rat hind paw representation before (**a**) and after (**b**) ICMS, as found in an electrophysiological experiment (*left*) and in the simulation (*right*). Cutaneous RFs (*dark areas*) are drawn for each selected cortical penetration site on a diagram of the hind paw. Blood vessels are shown as *gray lines* (*left*). The ssRF is marked by a *black rectangular frame* (*left* and *right*). The functional boundary between SI and motor cortex is marked as a dotted line and the reorganizational shift as a *bold line*

2.2.3 PPTS-induced cortical plasticity. Application of 6–12 h of PPTS on selected digits or pads caused substantial

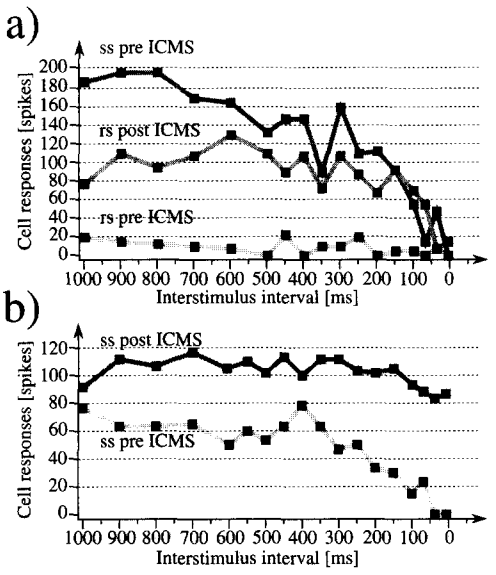

Fig. 3a,b. Characteristic examples of functional ICMS reorganization. **a** An interstimulus interval variation for tactile stimulation in an ssRF before ICMS does not generate an rs response above spontaneous activity (*rs pre ICMS*). After ICMS the rs activity to ssRF stimulation shows an attenuated low-pass response (*rs post ICMS*) similar to the one displayed by the ss before ICMS (*ss pre ICMS*). **b** The low-pass response at an ss before ICMS (*ss pre ICMS*) is changed into a nonspecific broadband response after ICMS (*ss post ICMS*)

changes and overall expansions of the respective skin representations (Godde et al. 1994, 1996; Dinse et al. 1995). The size of the cortical area representing the stimulated skin fields increased severalfold after PPTS, but retained its normal, low-threshold cutaneous characteristics. Enlarged RFs were predominantly found close to the stimulation sites but also up to 500 μm away.

This effect was selective in so far as the enlargement always comprised both stimulated skin fields. All effects were fully reversible 10–12 h after terminating PPTS. In contrast, following SPPS, no or only small changes were observed. To explore the potential perceptual consequences of PPTS-induced short-term plastic processes, we studied tactile spatial two-point discrimination performance in 22 human subjects. After 2–6 h of a PPTS protocol analogous to the above-described electrophysiological experiments, we found a significant improvement in spatial discrimination performance (Dinse et al. 1995).

3 Simulating short-term and reversible neuronal plasticity

3.1 The model hypotheses

The model we present here is based on six hypotheses about the underlying structure of the neural architecture as well as the nature of the observed plasticity.

When designing the architecture, we assume that:

•H1: the different neuronal stages existing between skin and cortex (dorsal column relay cells, ventroposterior thalamic relay cells, inhibitory coupling within reticular nucleus) can be functionally reduced to a single pre-cortical level.

This first hypothesis is required for simplification and to reduce the simulation time. A similar argument has been used in other simulations of plasticity (Grajski and Merzenich 1990; Favorov and Kelly 1994). The hypothesis does not modify the overall behavior of the network since we suppose that:

•H2: substantially less plasticity occurs at the pre-cortical level as far as the ICMS protocol is concerned.

This second hypothesis is due to the limited plasticity which can be induced by ICMS or intra-thalamic microstimulation at the thalamic level (Zepka et al. 1994). Following H1, we reduce the numerous stages of the subcortical pathway to a direct path between the hind paw skin and the "pre-cortical" stage of the model.

At the cortical level, the effects of ICMS were reported to have a maximal spatial extent of 800 μm (Spengler and Dinse 1994). This distance is assumed to be related to the size of the inter-columnar lateral projection of pyramidal cell axon collaterals (Gilbert and Wiesel 1981; Jones 1981) and inhibitory basket cells (Jones 1975). Therefore, we assume that:

•H3: topographical reorganization induced by ICMS/PPTS is mainly due to inter-columnar plasticity between cortical cells.

•H4: short-term plasticity induced by ICMS/PPTS especially affects excitatory connections between cortical pyramidal cells.

•H5: ICMS and PPTS effects are restricted in their spatial extents by distance-dependent boundaries of the synaptic plasticity range.

At present, our experimental data do not reveal direct evidence for the fourth hypothesis. However, synaptic plasticity is known to be mediated by excitatory N-methyl-D-aspertate (NMDA) receptors (cf. Kirkwood et al. 1993).

In H5, we assume that the synaptic density in a given cortical dendritic arborization decreases monotonically with the distance from its soma, according to a Poisson-like distribution (Abeles 1991; Hellwig et al. 1994). Moreover, it has been shown that the dendritic arborization density falls exponentially with increasing distance from the soma (Sholl 1956). We therefore consider that the possible variation in the amount of neurotransmitter released (i.e., the range of synaptic plasticity) is lower in the distal dendritic segments than in the more proximal ones.

To explain the functional changes observed in the tuning response of cortical cells after ICMS, it is necessary to assume that:

•H6: the somatosensory cortex shows a columnar organization in which intra-columnar and inter-columnar plasticity can differ.

This hypothesis is supported by experimental evidence in monkeys (Tommerdahl at al. 1993), cats (Favorov and Diamond 1990) and rats (Armstrong-James 1975; Lamour et al. 1983). However, column-like structures in the rat hind paw representation are not as distinct as the barrels found in the vibrissae representations. We consider columnar or maxicolumnar structures in the sense defined by Favorov and Diamond (1990): "columns" are groups of neurons distributed in a small cylindrical volume perpendicular to the brain surface with a diameter of 200–300 μm. The boundaries of such topographic entities can be detected by a dis-

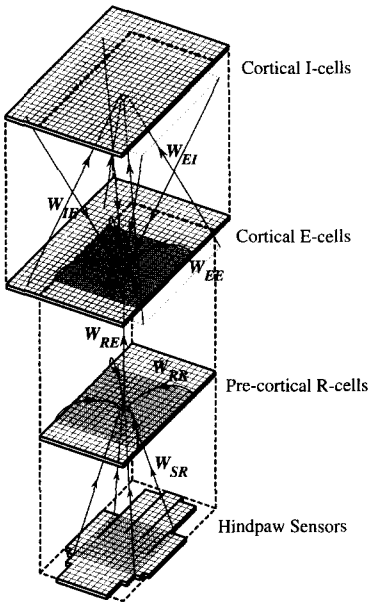

Fig. 4. Network architecture. Each *small square* represents a maxicolumn. The connections between receptive fields (*dark gray areas*) and neurons are indicated by *arrows*. W_{SR}, synaptic weights between sensors on the hind paw and thalamic relay cells, W_{RR}, lateral synaptic weights between thalamic relay cells, W_{RE}, synaptic weights between thalamic relay cells and excitatory cortical cells, W_{IE}, W_{EI}, synaptic weights between inhibitory and excitatory cells (*I-cells* and *E-cells*): W_{EE}, plastic lateral synaptic weights between E-cells

crete change in the position of the RF center (i.e., the minimal RF generating the strongest response) of cells located at both sides of the columnar boundary. Within a column, the position of the RF center remains constant but the RF surround geometry (i.e., the maximal RF generating a minimal response) may differ, as may the cells' response properties (Lamour 1983). We then consider "minicolumns" as radially oriented cell cords extending through layers II–VI, with an average center-to-center spacing of 30–50 μm (Tommerdahl et al. 1993). Within a minicolumn, the RF characteristics are nearly identical.

Without further specifications we use the word "column" synonymously with "maxicolumn".

3.2 The model architecture

The overall simulated architecture (Joublin et al. 1994) contains three main levels of information processing: the sensor array representing the hind paw skin, the pre-cortical relay cell array supposed to represent the different levels of excitatory and inhibitory relay cells and inhibitory nuclei up to the thalamus, and the array of cortical columns representing stellate, basket and pyramidal cell interactions (Fig. 4).

3.2.1 The sensor level. We simulate the hind paw skin by an array of 287 sensors (Fig. 4, bottom layer). The stimuli applied, $V_S(x, y)$, are gaussian distributions of spatial activities (1):

$$V_S(x,y) = A_T \cdot \exp\left[-\left((x-x_T)^2 + (y-y_T)^2\right)/\sigma_T^2\right] \quad (1)$$

with amplitude A_T ($A_T = 1$) at the target location (x_T, y_T) of the stimulus and various space constants σ_T, depending on whether the pre-cortical or cortical level was simulated (Fig. 5). Further details will be given in Sect. 3.3.1.

3.2.2 The pre-cortical level. As postulated in H1, we reduce the different intermediate levels between skin and cortex to a 15×25 array of relay cells. The afferent pyramid-like connectivity from the skin is modeled by a topographical connectivity defined by RFs[3] of 11×11 sensors with approximately 80% overlap. The overlap is large enough to allow competitive learning between neighboring relay cells.

The generation of a topographically ordered representation of the hind paw is modeled at the pre-cortical level in a separate step. This simplifies the simulation by introducing a dissociation between the map generation – probably occurring during the developmental stage of the animal (O'Leary et al. 1994) – and the post-ontogenetic plastic processes occurring at the cortical level. As the ontogenetic generation of cortical maps is beyond the scope of our simulations, we did not attempt to improve or discuss the chosen rules further. Other biologically relevant models are described in the literature (Favorov and Kelly 1994; Sirosh and Miikkulainen 1994).

Our goal is to generate a pre-cortical topography which takes into account the differences in RF sizes located on the heel, pads and toes of the rat hind paw to allow a detailed comparison with the experimentally recorded RFs before and after ICMS. We exploit a modified version of Kohonen's self-organizing map algorithm (Kohonen 1982) by using local input RFs and local neighborhoods for the "winner-take-all" final activation of the relay cells. The neighborhood RFs are chosen to be of 15×15 relay cells with an overlap of about 85% to allow local competition.

The refinement of the RF size and location during development is simulated using a range of stimuli which can be assumed to be found in the natural environment (Fig. 5a and Sect. 3.3.1). The learning rule and the shape of the input stimuli were chosen under the assumption that during ontogenesis competition takes place between synaptic connections (Parnavelas et al. 1988).

3.2.3 The cortical level. In agreement with H6, the cortical level representing the somatosensory cortex SI is simulated using an array of 21×29 maxicolumns. Maxicolumn in the model is defined as a set of minicolumns, and minicolumn as a subset of two main cells E and I (cell types defined later in this paragraph). This array is supposed to represent about $1.0\times1.4\,\text{mm}^2$ of cortex, comprising about $0.7\times1.2\,\text{mm}^2$ of somatosensory area and its border with the motor cortex. The anatomical boundary between these two cortical areas is defined by the type of efferent connections, arising exclusively from the pre-cortical structure for the somatosensory area. For simplicity, we studied the inter-columnar lateral plasticity by means of a single minicolumn per maxicolumn – reflecting the importance of inter-columnar plasticity for

[3] A cell RF in the model is the set of connections to the cell. It is similar to the dendritic arborization in the biological context.

the topographical reorganization (H3). Within this minicolumn, we consider four types of biological cells:

•Excitatory spiny stellate cells of layer IV (also ss-cells) which receive pre-cortical activity. The lateral extension of their dendritic arborization is limited to a few neighboring minicolumns (< 50 μm) (Jones 1981). Accordingly, this arborization alone is not sufficient to explain the spatial extent of plastic changes induced by ICMS. The spiny stellate cells send their axons into the supragranular layers in a narrow cylinder that embraces the apical dendrites of pyramidal cells located in the same minicolumn. For convenience, they are not directly simulated in the network and can be considered to be the pre-cortical input of the cortical excitatory E-cells.

•Excitatory pyramidal cells of layers II–V, which have apical dendrites through nearly all layers and basal dendrites that extend to 300–500 μm (Mountcastle 1978). Layer V pyramidal cells receive in particular dense cortico-cortical terminations from adjacent cortical regions (Guise and Chapin 1986). These cells are modeled as excitatory cells (E-cells) with small RFs.

•Inhibitory basket cells of layer III or V, whose axons form dense nets around pyramidal cell bodies and project horizontally up to 1 mm (Marin-Padilla 1974). Their dendritic trees are moderately spiny and receive collateral pyramidal axons. They can simultaneously affect cells situated at any depth in neighboring columns. They are supposed to mediate inhibition adjacent to the columns which are excited by peripheral stimulation (Mountcastle and Powell 1959). We model these cells as inhibitory cells (I-cells) with large RFs.

•Inhibitory double bouquet cells whose axons form dense vertical curtains in layers II and V. They receive input from spiny stellate cells and inhibit pyramidal cells in neighboring minicolumns. These cells are not simulated in the RF reorganization experiment because they do not influence it, but they are important for the functional aspects of the reorganization (see Discussion).

The previously described I- and E-cells are connected in the model in different ways: E-cells receive direct input from pre-cortical relay cells in a one-to-one scheme so that no new topography is generated between the pre-cortical and cortical level. To control the temporal patterns of activity produced by the flow of sensory information, reciprocal connections between E- and I-cells are required. From the four theoretically possible pathways between E- and I-cells, we consider only three (E to I, I to E, E to E). Adding connections between I-cells has no qualitative effects on the outcome of the simulations. The extent of the excitatory neighborhood (E to E) is restricted to the extent of the basal horizontal dendrites of pyramidal cells and is chosen to be 15×15 units. The extent of the connectivities of both E- to I-cells and I- to E-cells is taken to cover the range observed for basket cells, which represents about 1 mm^2 or 21×21 units in the simulation. In all cases, the given sizes correspond to the potential connectivity, but do not represent the entire, experimentally observed RF size, which is assumed to depend on the synaptic strength and on the amount of lateral inhibition.

3.2.3.1 Activation rules. The overall behavior of the simulated cortical cells follows the dynamics of Wilson and Cowan's (1973) model. The membrane potential of both E- and I-cells is defined by an additive rule (2):

$$\left.\begin{aligned} U_{E_j}(t) &= V_{R_j} + \sum_{(k\in\mathscr{R}_{EE}(j),k\neq j)} W_{E_k,E_j}(t)\cdot V_{E_k}(t) \\ &\quad - \sum_{i\in\mathscr{R}_{IE}(j)} W_{I_i,E_j}(t)\cdot V_{I_i}(t) \\ U_{I_i}(t) &= \sum_{j\in\mathscr{R}_{EI}(i)} W_{E_j,I_i}(t)\cdot V_{E_j}(t) \end{aligned}\right\} \quad (2)$$

with $\mathscr{R}_{EE}(j)$ the index set representing the neighborhood RF of E-cell j, $\mathscr{R}_{IE}(j)$ the index set representing the RF of E-cell j coming from I-cells, $\mathscr{R}_{EI}(i)$ the index set representing the RF of I-cell i coming from E-cells, $W_{E_k,E_j}(t)$ the synaptic weight between E-cell k and E-cell j, $W_{I_i,E_j}(t)$ the synaptic weight between I-cell i and E-cell j, $W_{E_j,I_i}(t)$ the synaptic weight between E-cell j and I-cell i, and $V_{R_j}(t)$, $V_{E_j}(t)$, $V_{I_i}(t)$, respectively, the activity of pre-cortical relay cell j, of E-cell j and of I-cell i. $V_{R_j}(t)$ is the result of local competition within the lateral RF of the pre-cortical relay cells. This competition takes place after the computation of the feedforward weighted sums of the hind paw sensor activities.

The dynamical behavior of both E- and I-cells results from the following differential equations (3):

$$\left.\begin{aligned} \tau_E\cdot\dot{V}_{E_j}(t) &= -V_{E_j}(t) + \big(1-\gamma_E\cdot V_{E_j}(t)\big) \\ &\quad \cdot f_{\theta_E,\eta_E}(\tau_E\cdot U_{E_j}(t)) \\ \tau_I\cdot\dot{V}_{I_i}(t) &= -V_{I_i}(t) + \big(1-\gamma_I\cdot V_{I_i}(t)\big) \\ &\quad \cdot f_{\theta_I,\eta_I}(\tau_I\cdot U_{I_i}(t)) \end{aligned}\right\} \quad (3)$$

where τ_E, τ_I represent the membrane time constants of each cell and γ_E, γ_I represent the refractory periods of the cells. $\dot{V}$ is the first time derivative of V. The non-linear function $f_{\theta,\eta}(U)$ is chosen to be a sigmoid (4) with θ_E, θ_I being the thresholds of the cells (points of inflection of the sigmoid) and η_E, η_I the slopes of the sigmoids.

$$f_{\theta,\eta}(U) = \big\{[(1+\exp(-\eta(U-\theta))]^{-1} - N)/(1-N)\big\}^{+} \quad (4)$$

where $N = (1+\exp(-\eta\theta))^{-1}$ and $[x]^{+}$ stands for x if $x > 0$ and 0 otherwise.

This type of differential equation (3) presents three different modes of dynamics depending on the value of the parameters (Wilson and Cowan 1973). The parameters of the simulations were chosen to obtain an "active transient mode" (Table 1). In this mode, the response to a stimulus restricted in space, time and intensity, continues to increase after the stimulus has ceased until reaching a maximum and then decays back to a resting state (which we refer to as spatio-temporal integration).

3.2.3.2 Learning rules. The interaction between E- and I-cells influences the size of their RFs, as observed by Armstrong-James (1975) and Chapin and Lin (1992). However, according to H2, H3 and H4, we assume that most of the observed reorganization is due to plasticity between E-cells in cortex. We modeled this hypothesis at a macroscopic level by allowing modifications of weights between E-cells according to (5) and (6). The weights from E- to I-cells and vice versa are left constant.

$$M_{jk}(t) = (1+\gamma_E)\max\big(V_{E_j}(t), V_{E_k}(t)\big) - \varepsilon \quad (5)$$

$$\left.\begin{aligned} M_{jk}(t) \geq 0, \Delta W_{E_j,E_k}(t+\Delta t) &= \alpha^{+}_{EE} \cdot M_{jk}(t) \\ &\cdot \left(W^{max}_{E_j,E_k} - W_{E_j,E_k}(t)\right) \\ M_{jk}(t) < 0, \Delta W_{E_j,E_k}(t+\Delta t) &= \alpha^{-}_{EE} \cdot M_{jk}(t) \\ &\cdot \left(W^{min}_{E_j,E_k} - W_{E_j,E_k}(t)\right) \end{aligned}\right\} \quad (6)$$

where ε is an activity threshold, α^{+}_{EE}, α^{-}_{EE} are respectively constant learning and unlearning rates, and $W^{min}_{E_j,E_k}$, $W^{max}_{E_j,E_k}$ are respectively the lower and upper boundaries of the weights between E-cells j and k. $M_{jk}(t)$ is the normalized maximal amount of pre- or postsynaptic potential above the threshold ε.

The first equation (5) states that a minimum level ε of pre- or postsynaptic activation is needed to initiate learning. Unlearning occurs when both pre- and postsynaptic levels are below the threshold ε. The choice and the interpretation of this not-strictly-Hebbian rule is discussed in the last part of this paper.

Equation (6) gives, dependent on the sign of M_{jk}, the weight changes for learning and unlearning. The last part of each equation allows the synaptic strength to stay within predefined boundaries. This serves firstly to avoid unsteadiness in the cortical map and secondly to allow the effects of reversibility. During ICMS, learning and spatio-temporal integration spread increasing activity into the neighborhood of the ss-cell, enabling the extension of RFs as observed in the experiments.

According to H5, we define the synaptic strength of all connections by gaussian distributions. The modifiable synaptic weights between E-cells are bounded by two such distributions (6), whereas synaptic weights with inhibitory cells remain constant. The different distributions are defined by their amplitudes A_{EI}, A_{IE}, A_{EE} and space constants σ_{EI}, σ_{IE}, σ^{max}_{EE}, σ^{min}_{EE} respectively for W_{EI}, W_{IE}, W^{max}_{EE}, W^{min}_{EE}. According to Wilson and Cowan (1973), the space constants are chosen to ensure that no uniformly excited state can emerge in the absence of maintained stimulation, and the excitatory to inhibitory interactions are longer ranging than excitatory to excitatory interactions:

$$\sigma_{EI} > \sigma^{max}_{EE} > \sigma^{min}_{EE} \quad (7)$$

3.3 Simulation results

3.3.1 Set-up of the pre-cortical topography. As noted before, the pre-cortical stage enables us to generate a topographically ordered representation of the hind paw on the cortex (called a map). This important processing step is based on the connection tree that links the skin to the cortex and on the local computations within the cortex. However, to simplify the model and to try to separate the ICMS effects from ontogenetic and developmental aspects, we have implemented the map at the pre-cortical level only.

To generate the pre-cortical interconnection map with the cortical structures, we set up a model of hind paw stimuli related to the rat's walking patterns. During walking, the stimulated skin surface is much larger for the heel than for the toes, and the toes can be moved fairly independently of each other. Thus, the probability of having two neighboring

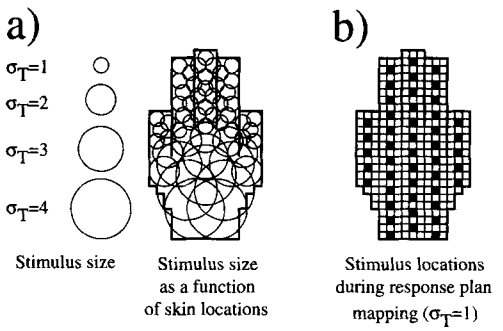

Fig. 5a,b. Simulated tactile stimulation protocol. **a** Distribution of the stimulus size as a function of the position on the hindpaw. **b** *Small black squares* represent the positions of stimuli used for the generation of the cortical RF representation

spots stimulated simultaneously is much greater on the heel than on the toes. We therefore generated stimuli with spatial extents (i.e., space constants) dependent on their locations on the hind paw . Such gaussian stimuli were randomly chosen over the simulated hind paw during 4000 cycles. With this procedure, we are able to generate RFs with a size gradient along the distal-proximal axis of the paw (Fig. 5a).

After the setting up of the pre-cortical topography, which had to be achieved before the ICMS experiments, no further learning was allowed at this level.

3.3.2 Topographical RF reorganization. The main goal was to investigate whether our hypotheses and assumptions are sufficient to explain the reorganizational changes, including the aspects of reversibility induced by ICMS.

3.3.2.1 Simulation protocols. Two main protocols are employed in the simulations: the first one is used to simulate the ICMS protocol of repetitive and highly synchronous enforced firing, the second one is aimed at determining the locations and sizes of RFs in the cortex, comparable to the "mapping" procedure in the biological experiments. Simulations are processed at different time scales.

Cortical RFs are determined using a protocol close to the biological mapping procedure. We choose 46 points on the hind paw skin (Fig. 5b), which are stimulated for 8 ms. The ISI is 100 ms in order to allow the network to reach a steady state. One cycle of the simulation corresponds to dt = 1 ms real time and 4600 cycles are needed to apply all the stimuli. Each skin stimulation covers about 4 mm^2 skin surface (simulated hind paw of 10 × 17 mm^2 or 15 × 25 columns). For each hind paw stimulation, we obtain a cortical map of activity (i.e., magnification). All these maps are combined to reconstruct RFs at each skin point and these points are then interpolated to obtain the RF maps as illustrated in the right-hand part of Fig. 2.

ICMS stimuli are simulated by forcing a high activity on the pre-cortical input (V_R) of the ss E-cell. Because of time constraints (1 ms in biological experiments corresponds to about 0.5 s of simulation on a Sun Sparc 2), it is not possible to simulate 2 or 3 h of ICMS at a resolution of 1ms. Instead, we overamplified the effect of plasticity to reduce

Table 1. Simulation parameters for the cortical level

σ_{EI}	20	σ_{IE}	5.0
σ_{EE}^{max}	4.0	σ_{EE}^{min}	1.0
A_{EI}	0.5	A_{IE}	0.5
A_{EE}	1.5	ε	0.5
α_{EE}^{+}	1.0	α_{EE}^{-}	0.01
τ_E, τ_I	1 ms	γ_E, γ_I	10 ms
θ_E	9.0	θ_I	17.0
η_E	0.5	η_I	0.3

simulation time to generate the pre-cortical representation. Learning is accelerated by choosing a learning rate α_{EE}^{+} of 1. The RF reorganization converges after ten stimuli of eight cycles each on ss-cells with an ISI of 100 cycles (Fig. 2b, right). Simulations have shown that this time scaling does not affect the qualitative results, but does enable us to estimate the biological learning rate which is calculated to be in the range of about 10^{-4} (assuming that the stimulation time is inversely proportional to the learning rate that would give $10 \times 100/2 \times 3600$). As described above, the ICMS-induced plasticity is fully reversible. We introduced an unlearning rate α_{EE}^{-} (6) with a value about 100 times smaller than α_{EE}^{+}. Unlearning occurs only when the cell activity is smaller than the threshold $\varepsilon(\varepsilon = 0.5)$. Indeed, due to the temporal aspects of the cell responses, the time period, during which the activity is greater than ε, is much shorter than the time period during which the activity is smaller than ε.

3.3.2.2 RF expansion and reversibility. Using the simulation parameters described above (Table 1), we obtained results which were remarkably in accordance with the experimentally described effects. During ICMS, the rsRFs progressively increased in the direction of the pre-ICMS ssRF (Fig. 2, right). RF sizes appear to be generally smaller in the simulation than in experiments. This effect is controlled by two parameters. The first is the size of the patterns used to stimulate the skin sensors during the generation of the pre-cortical topographical map (Fig. 5). We used stimuli not larger than a quarter of the hind paw which is certainly much smaller than the stimulation patterns encountered during walking. The other parameter is the space constant σ_{EE}^{max} of the gaussian distribution used as boundary for the excitatory weights. Increasing this parameter leads to an increase in the activity around ss and consequently to an enlargement of RF representations. We chose a value for σ_{EE}^{max} which produces some elongated RFs towards ss, as was typically observed in the biological experiment. We examined in more detail one parameter of this extension: the degree of RF overlap between the pre-ICMS ssRF and the post-ICMS rsRF. Figure 6 shows the similarity in the distributions of the simulated and experimental overlap data. The main difference between the two distributions is found at an overlap of 75%, but this gap already exists pre-ICMS in the experimental data. Overlaps of 75% do not appear in the simulations, probably because the RFs pre-ICMS were too small (cf. previous explanation).

We also observed a reversibility of RF changes in the simulated ICMS effects, as can be predicted from our equations. These effects are due to the rate of the "unlearning"

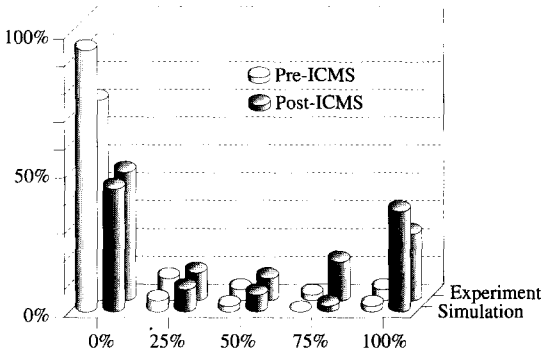

Fig. 6. Degree of overlap between ss-RF pre-ICMS and rs-RF pre- or post-ICMS for both the experimental data and the simulation results

process and to the pre-defined limits of weights. The lower weight limits allow the return to a RF organization similar to that found under control conditions without requiring tactile stimulation, as is the case in the biological experiments.

Although not explicitly intended in our model, we were able to simulate the functional relocation of the areal and modality boundaries. The anatomical boundary was modeled by restricting pre-cortical inputs to the somatosensory cortical area, thus prohibiting external inputs to the neighboring region of the motor cortex. Without altering the running and learning rules, the previously non-somatosensory regions developed responses to tactile stimulation because of the ICMS-induced reorganization of RFs across the areal and modality boundaries (Fig. 2).

4 Discussion

4.1 Different learning rules underlying different forms of plasticity

The ICMS and the PPTS stimulation protocols revealed significant reorganizational processes at the cortical level. In the PPTS experiments, temporally coherent inputs were provided by the associative pairing of simultaneously applied tactile stimulation at two different skin sites, which opens the possibility of studying, in vivo, constraints on learning rules. When, however, instead of two stimuli only a single selected skin location was stimulated for several hours (single point peripheral stimulation, SPPS), no or only very small changes were observed (B. Godde and H.R. Dinse, unpublished observations). From the perspective of the number of sites that are activated, the ICMS is comparable to the SPPS protocol, but ICMS revealed dramatic changes, while SPPS did not induce cortical reorganization. To account for this differential effectiveness, we assume different learning rules acting within the columnar system. In the ICMS experiments, a non-Hebbian rule depending on either pre- or post-synaptic activity is postulated to explain the topographical reorganization of RFs due to synaptic enhancement. Two possible mechanisms may be involved. First, following the operation of a Hebbian rule, a synaptic enhancement over a small "volume" can be assumed (Bredt and Snyder 1992; Edelman and Gally 1992; Montague and Sejnowski 1994). Second, according to the so-called DYSTAL rule (for DYnamicallly STable Associative Learning), two synapses on

a common neuron are strengthened if both received pre-synaptic stimulation for two consecutive time steps (Alkon et al. 1994). It should be noted that during recent years experimental evidence for non-Hebbian synaptic mechanisms has been accumulating (Alonso et al. 1990; Kossel et al. 1990; Granger et al. 1994).

In the case of PPTS, two pyramidal cells are stimulated simultaneously and a local Hebbian rule or DYSTAL rule between middle range cortical connections and thalamic inputs can easily explain the mutual reinforcement of the connectivity between cells (Fig. 7a). The enlargement of the pyramidal RF in direction of the other pyramidal cell can be explained in this case by a DYSTAL rule occurring at the level of intermediate pyramidal cells receiving afferents from both stimulated cells.

In the case of ICMS, a combination of DYSTAL and Volume Hebbian rules is sufficient to simulate a spatial extent of the observed effects up to 800 μm. The DYSTAL rule in the neighborhood of the ss-cell involves pre-synaptic connections from ss-cell and connections (Fig. 7b) of the thalamic axonal arborizations (with average radius of about 500–600 μm, cf. Jensen and Killackay 1987), antidromically activated. The Volume Hebbian rule proceeds at each pyramidal cell affected by the preceding reorganizational step. The artificial nature of ICMS can induce a DYSTAL learning via (i) antidromic activation of the thalamic axonal arborizations reaching layer IV and (ii) antidromic activation of cortical axon collaterals whose extent covers at least 800–1000 μm and whose density is even higher than that of thalamic fibers. Such a mechanism cannot come into play when a SSPS is performed (Fig. 7a, c). It has been reported that the spatial extent of current spread during ICMS, a 10 μA pulse of cathodal current, activates neurons within 80–100 μm around the stimulation site in primate motor cortex (Stoney et al. 1968). Evidence for an involvement of antidromic components during ICMS has recently been provided using cortical slice preparations (Heusler et al. 1995).

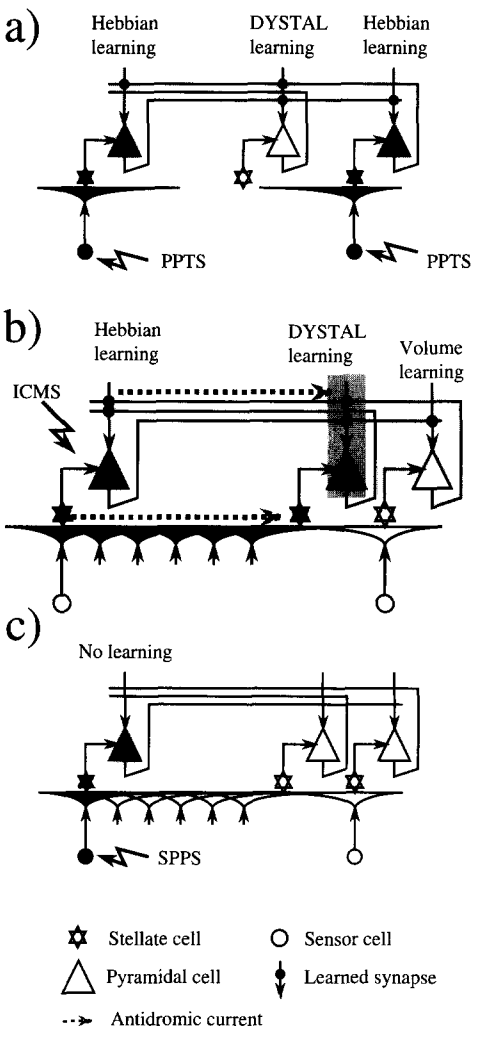

Fig. 7a–c. Proposed mechanisms of ICMS, PPTS and SPPS effects. **a** PPTS: middle-range connections are reinforced due to synchronous pre-cortical input synapses. A spread of activation is due to the synchronization of hybrid inputs (DYSTAL rule). **b** ICMS: the highly synchronizing effect of ICMS activates fibers antidromic, which in turn affect pyramidal cells using the DYSTAL rule. **c** SPPS: tactile stimulation on a single skin site is not sufficient to induce a DISTAL activation. Consequently, no reorganization takes place

4.2 Functional reorganization of single cell transfer properties

To understand possible mechanisms underlying the changes in the transfer characteristics of cortical neurons, we analyzed the organization of the cortical microcircuitry in detail. According to our hypothesis (H6), the activity of the cells results from two types of interactions: i) those within the minicolumn or with its neighboring minicolumns within a maxicolumn, and ii) those between maxicolumns. Each minicolumn in a maxicolumn is supposed to have different frequency and intensity characteristics, due to different tuning properties of the single cells.

Figure 7 depicts the model of the connectivity within the somatosensory cortex that we use to explain the experimental results. During ICMS, as seen in Sect. 3.2.3, the pathway between the stimulated pyramidal cell of a maxicolumn and minicolumns in neighboring maxicolumns is reinforced (black dots on the horizontal and vertical bold lines connected with the ss-pyramidal cell in Fig. 8). This bidirectional pathway enables the enlargement of both ssRF and rsRF as described before. The reinforced link between ss- and rs-pyramidal cells is assumed to be responsible also for the transfer of the tuning characteristics of the ss-stellate cell to the rsRF. As a consequence, the low sensibility of the rs-cells for ssRF stimulation pre-ICMS (dotted arrow at the bottom of Fig. 8 coming from the pre-cortical level) is replaced after ICMS by the response properties of the ss-stellate cell. Another mechanism is postulated to occur inside the maxicolumn: in this case we assume a reinforcement of the connections between stellate cells of minicolumns in the ss neighborhood, and the ss-stellate cell (bold arrows on the ss-stellate cell in Fig. 8). The ss-stellate cell then incorporates the tuning responses of its neighbors, which results in an increase of its tuning bandwidth. This local interaction between stellate cells is probably compensated at the ss-pyramidal cell by the inhibitory interactions of ss-neighbor double bouquet cells, so that the rs tuning becomes fairly similar to the ss pre-ICMS tuning. This is compatible with

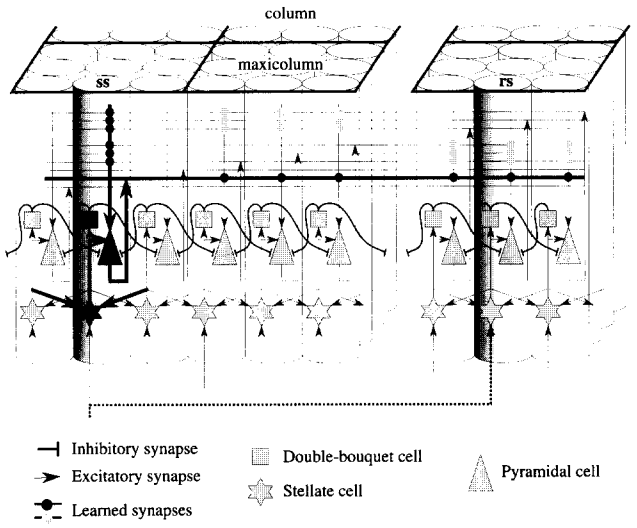

Fig. 8. Columnar connectivity scheme of SI. Each *cylinder* represents a minicolumn. These minicolumns are clustered in a maxicolumnar structure. The two *shaded minicolumns* correspond to the ss and rs, respectively. Each minicolumn contains four types of cells: spiny stellate cell (*star*), pyramidal cell (*triangle*, E-cell) and double bouquet interneuron (*square*): for simplicity the basket inhibitory cells (I-cells) are not included. The main pathways on which learning occurs are depicted with *bold lines*. The excitatory weights modified during ICMS (*black and gray dots*) are lined up horizontally and vertically between the ss and intra- or extra-columnar recording sites. The stellate cell in each column is characterized by cell-specific frequency and intensity transfer characteristics different from those of other stellate cells in the same maxicolumn

previous models of a columnar organization (Favorov and Kelly 1994).

4.3 Interpretation of ICMS- and PPTS-induced plasticity

One of the main differences between the two experimental protocols is that PPTS involves the entire sensory pathway. Therefore, plastic changes can occur to various degrees at cortical and subcortical levels. In contrast, the ICMS protocol offers the advantage of investigating locally in acute experiments the capacities and constraints of functional plasticity, regardless of effects from the sensory periphery and the ascending pathways. It has been utilized to study plasticity of areal borders, laminar-specific and thalamic-specific ICMS plasticity (Spengler and Dinse 1994; Shuishi-Haupt et al. 1994; Zepka et al. 1994). Assuming that both ICMS and PPTS are capable of generating reorganization of RFs and representational maps, one open question is how these changes are related to strategies of information processing. In other words, what is the impact of short-term neuronal reorganization in primary sensory representations on information processing and, consequently, on behavioral and perceptual performances?

Although in this respect ICMS must be regarded as an artificial tool, its use for stimulation of direction selective neurons in MT visual cortex during a motion detection task changed the animals' judgments towards the direction of motion encoded by the stimulated neurons, indicating that ICMS can directly influence behavior (Salzman et al. 1990).

There are a number of studies that report a direct relationship between improved perceptual abilities and map reorganization on different time scales. Human Braille readers were shown to have an enlarged sensory representation of the reading finger (Pascual-Leone and Torres 1993). Prolonged behavioral training in a tactile and auditory frequency discrimination task revealed striking cortical reorganizations parallel to improved discrimination thresholds (Recanzone et al. 1992a,b, 1993). Human psychophysical experiments in the visual system related to hyperacuity revealed rapid perceptual learning capabilities which raise the question of fast parallel changes of cortical organization (Poggio et al. 1992; Kapadia et al. 1994). Old rats (> 24 months) have been reported to show a striking degradation of their cortical organizations compared with young animals (Spengler et al. 1995). These changes were correlated with deficits in limb coordination and decreased motor activity. It is assumed that age-related sensorimotor decline generates modified sensory inputs and that their impact is causally related to the breakdown of cortical representational topographies. Together, this means that experience or use/disuse are crucial factors which affect the idiosyncratic layout of cortical representations.

Remarkably, the PPTS protocol was similarly effective at the perceptual level by enhancing the spatial discrimination performance. This suggests that the fast plastic processes discussed have perceptual consequences, supporting the significance of cortical reorganizational processes. At first sight, the enhancement of the discrimination performance might appear surprising in view of the reported receptive field enlargement. However, perceptual thresholds are usually lower than corresponding thresholds of single neurons. Hyperacuity, for example, can not be explained on the basis of concepts of RF sizes of single cells. The observed changes in cortical response properties included map reorganization and an increase of RF overlap as a consequence of RF enlargement, and thus an increase in the number of neurons activated by stimulating a selected skin site. Concomitantly, the response duration became longer, increasing the time over which the neurons are active. It is conceivable that all these changes taken together can account for enhanced spatial discrimination. This hypothesis has much in common with the "coarse coding principle" (Hinton et al. 1986; Baldi and Heiligenberg 1988; Eurich et al. 1994). This principle was established to explain the frequently observed broad tuning properties or large RF sizes which nonetheless allow a fine discrimination on a behavioral level by populations of neurons. Theoretical analysis of our rat data in the framework of coarse coding predicts a 30%–40% increase of the spatial resolution of the stimulated skin sites (H. Schwegler, C. Eurich, U. Dicke, B. Godde and H.R. Dinse, in preparation), which matches with the range of improvement observed in our PPTS psychophysical experiments in humans.

In addition, our experiments were restricted to a primary cortical area and there are as yet no data about parallel changes in higher areas. Such changes could decisively contribute to an enhancement of perceptual performances, as we found after a few hours of PPTS by humans.

5 Conclusions

We compared different stimulation protocols (ICMS, PPTS, SPPS) which induced different forms and degrees of plastic changes. Using our simulations and assumptions in the framework of a columnar model, we revealed the importance of the interactions of different Hebbian learning rules. These rules are Hebbian-like in the sense that they result in the mutual strengthening of coincident or nearly coincident inputs, but differ in other properties. From a more general point of view, the input-related plasticity in SI can be interpreted as a process of self-organization of computational resources to adapt use-dependent representation to a limited cortical area. Accompanying changes of correlated activity suggest that, in addition to the gain in neuron number, a higher and more effective processing might be achieved by parallel alterations of the temporal structure and of the degree of synchronization between neurons (Ahissar et al. 1992; Dinse et al. 1990, 1993). It appears reasonable that these changes enable higher levels to perform a faster and more elaborate decoding and processing of information. However, it remains an open question how higher cortical levels can use and decode plastic representational changes that are due to ongoing changes of their input sources without jeopardizing the stability of processing and representation.

Acknowledgements. This work was supported by the Deutsche Forschungsgemeinshaft (DFG, Germany), grants from Région Haute-Normandie (France) and from the Deutscher Akademischer Austauchdienst (DAAD, Germany) and the Institut für Neuroinformatik. We thank Prof. Dr. von Seelen for extensive discussions on cortical plasticity and for providing us with a stimulating environment that brings together theory and experiment. We also appreciated the critical suggestions and comments on an earlier version of the manuscript by Dr. P. Bedenbaugh, Dr. B. Wright, Dr. C. Schreiner and the anonymous reviewers. We gratefully acknowledge the contributions of B. Godde, Dipl. Biol., to the PPTS experiments and the work of Roberto F. Zepka, Dipl. Biol., regarding thalamocortical plasticity. We also thank W. Erlhagen, Dipl. Math., for valuable discussions on the work of Wilson and Cowan. Part of this work was done at the LCIA/La3i at the University of Rouen, France.

References

1. Abeles M (1991) Corticonics: neural circuits of the cerebral cortex. Cambridge University Press, Cambridge pp 81–91
2. Ahissar E, Vaadia E, Ahissar M, Bergman H, Arieli A, Abeles M (1992) Dependence of cortical plasticity on correlated activity of single neurons and on behavioral context. Science 257:1412–1415
3. Alkon DL, Blackwell KT, Barbour GS, Werness SA, Vogl TP (1994) Biological plausibility of synaptic associative memory models. Neural Networks: 7:1005–1017
4. Alonso A, Curtis M de, Llinas R (1990) Postsynaptic Hebbian and non-Hebbian long-term potentiation of synaptic efficacy in the entorhinal cortex in slices and in the isolated adult guinea pig brain. Proc Natl Acad Sci USA 87: 9280–9284
5. Andres M, Schlüter O, Spengler F, Dinse HR (1994) A model of fast and reversible representational plasticity using Kohonen mapping. In: Marinaro M, Morasso PG (eds) Proc Int Conf on Artificial Neural Networks ICANN'94. Springer, Berlin Heidelberg New York, pp 306–309
6. Antonini A, Stryker MP (1993) Rapid remodeling of axonal arbors in the visual cortex. Science 260: 1819–1821
7. Armstrong-James M (1975) The functional status and cortical organization of single cells responding to cutaneous stimulation in neonatal rat somatosensory cortex SI. J Physiol (Lond) 246: 501–538
8. Baldi P, Heiligenberg W (1988) How sensory maps could enhance resolution through ordered arrangements of broadly tuned receivers. Biol Cybern 59: 313–318
9. Bedenbaugh PH, Maldonado PE, Gerstein GL (1992) Comparative plasticity of somatosensory and auditory cortex in rat. Soc Neurosci Abstr 18: 346
10. Bredt DS, Snyder SH (1992) Nitric oxide, a novel neuronal messenger. Neuron 8: 3–11
11. Burnod Y (1988) An adaptive neural network: the cerebral cortex. Masson, Paris
12. Chapin JK, Lin CS (1992) The somatic sensory cortex of the rat. In: Kolb B, Tees R (eds) The cerebral cortex of the rat. MIT Press, Cambridge, Mass, pp 341–380
13. Darian-Smith C, Gilbert CD (1994) Axonal sprouting accompanies functional reorganization in adult cat striate cortex. Nature 368: 737–740
14. Dinse HR, Recanzone G, Merzenich MM (1990) Direct observation of neural assemblies during neocortical representational reorganization. In: Eckmiller R, Hartmann G, Hauske G (eds) Parallel processing in neural systems and computers. Elsevier, Amsterdam, pp 65–70
15. Dinse HR, Recanzone GH, Merzenich MM (1993) Alterations in correlated activity parallel ICMS-induced representational plasticity. Neuroreport 5: 173–176
16. Dinse HR, Spengler F, Godde B (1995) Short-term plasticity of topographic organization of somatosensory cortex and improvement of spatial discrimination performance induced by an associative pairing of tactile stimulation. Institut für Neuroinformatik, Ruhr Universität, Bochum. (Internal report INI 01-95), pp 1–8
17. Edelman GM, Gally JA (1992) Nitric oxide: linking space and time in the brain. Proc Natl Acad Sci USA 89: 11651–11652
18. Eurich C, Schwegler H, Strohmeier M (1994) Coarse coding: Die Berechnung des Aufloesungsvermoegens von Ensembles breitbandig abgestimmter McCulloch-Pitts-Neuronen. ZKW-Bericht no.6/94. Zentrum für Kognitionswissenschaften, University of Bremen
19. Eysel UT (1992) Remodelling receptive fields in sensory cortices. Cur Opin Neurobiol 2: 389–391
20. Favorov OV, Diamond ME (1990) Demonstration of discrete place-defined columns – segregates – in the cat SI. J Comp Neurol 298: 97–112
21. Favorov OV, Kelly DG (1994) Minicolumnar organization within somatosensory cortical segregates. I. Development of afferent connection. Cerebral Cortex 4: 408–427
22. Garraghty PE, Kaas JH (1992) Dynamic features of sensory and motor maps. Cur Opin Neurobiol 2: 522–527
23. Gilbert CD, Wiesel TN (1981) Laminar specialization and intra-cortical connections in cat primary visual cortex. In: Schmidt F, et al (eds) The organization of the cerebral cortex. MIT Press, Cambridge, Mass
24. Gilbert CD, Wiesel TN (1992) Receptive field dynamics in adult primary visual cortex. Nature 356: 150–152
25. Godde B, Spengler F, Dinse HR (1994) Hebbian pairing of tactile stimulation. I. Cortical physiology: rapid topographic reorganization of somatosensory cortex of adult rats. Soc Neurosci Abstr 20: 1429
26. Grajski KA, Merzenich MM (1990) Neural network simulation of somatosensory representational plasticity. In: Touretzsky DS (ed) Advances in neural information processing systems, vol. 2 Morgan-Kaufmann, pp 52–59
27. Granger R, Whitson J, Larson J, Lynch G (1994) Non-Hebbian properties of long term potentiation enable high capacity encoding of temporal sequences. Proc Natl Acad Sci USA 91: 10104–10108
28. Guise JLU, Chapin JK (1986) Influence of local cortico-cortical circuits on layer V receptive fields in the rat SI barrelfield. Soc Neurosci Abstr 16:1433
29. Hebb OD (1949) The organization of behavior. Wiley, New York
30. Hellwig B, Schüz A, Aersten A (1994) Synapses on axon collaterals of pyramidal cells are spaced at random intervals: a Golgi study in the mouse cerebral cortex. Biol Cybern 71: 1–12
31. Heusler P, Böhmer G, Dinse HR (1995) Mechanisms involved in cortical plasticity induced by intracortical microstimulation (ICMS) of adult rat somatosensory cortex in vitro. Eur J Neurosci Suppl S8: 43

32. Hinton GE, McClelland JL, Rumelhart DE (1986) Distributed representations. In: Rumelhart DE, McClelland JL (eds) Parallel distributed processing, vol. 1. MIT Press, Cambridge, Mass, pp 77–109
33. Jensen KF, Killackay HP (1987) Terminal arbors of axons projecting to the somatosensory cortex of adult rat. I. The normal morphology of specific thalamocortical afferents. J Neurosci 7: 3529–3543
34. Jones EG (1975)Varieties and distribution of the non-pyramidal cells in the somatic sensory cortex of the squirrel monkey. J Comp Neurol 160: 205–268
35. Jones EG (1981) Anatomy of cerebral cortex: columnar input-output organization. In: Schmitt F, et al. (eds) The organization of the cerebral cortex. MIT Press, Cambridge, Mass, pp 199–235
36. Joublin F, Spengler F, Wacquant S, Dinse H (1994) Simulations of experimental results on somatosensory map reorganization induced by intra-cortical micro-stimulation. In: Halin J, Karplus W, Rimane R (eds) First joint conference of international simulation societies proceedings. Zurich, pp 562–566
37. Kaas JH, Krubitzer LA, Chino YM, Langston AL, Polley EH, Blair N (1990) Reorganization of retinotopic cortical maps in adult mammals after lesion of the retina. Science 248: 229–231
38. Kapadia MK, Gilbert CD, Westheimer G (1994) A quantitative measure for short-term cortical plasticity in human vision. J Neurosci 14: 451–457
39. Kirkwood A, Dudek SM, Gold JT, Aizenman CD, Bear MF (1993) Common forms of synaptic plasticity in the hippocampus and neocortex in vitro. Science 260: 1518–1521
40. Kohonen T (1982) Self-organized formation of topologically correct feature maps. Biol Cybern 43: 59–69
41. Kossel A, Bonhoeffer T, Bolz J (1990) Non-Hebbian synapses in rat visual cortex. Neuroreport 1: 115–118
42. Lamour Y (1983) Etude de l'organisation laminaire du cortex somesthésique primaire du rat. Doctoral thesis, Université Pierre et Marie Curie, Paris VI, France
43. Lamour Y, Guilbaud G, Willer JC (1983) Rat somatosensory (Sml) cortex. II. Laminar and columnar organization of noxious and non-noxious inputs. Exp Brain Res 49: 46–54
44. Marin-Padilla M (1974) Three dimensional reconstruction of the pericellular nests (baskets of the motor-area 4- and visual-area 17-areas of the human cerebral cortex): a Golgi study. Z Anat Entwickl-Gesch 144:123–135
45. Merzenich MM, Sameshima K (1993) Cortical plasticity and memory. Cur Opin Neurobiol 3: 187–196
46. Merzenich MM, Nelson RJ, Stryker MP, Cynader MS, Schoppmann A, Zook JM (1984) Somatosensory cortical map changes following digit amputation in adult monkeys. J Comp Neurol 224: 591–605
47. Montague PR, Sejnowski TJ (1994) The predictive brain: Temporal coincidence and temporal order in synaptic learning mechanisms. Learning Memory 1: 1–33
48. Mountcastle VB (1978) An organizing principle for cerebral function: the unit module and the distributed system. In: Schmitt FO (ed) The mindful brain. MIT Press, Cambridge, Mass., pp 7–50
49. Mountcastle VB, Powell TPS (1959) Neural mechanisms subserving cutaneous sensibility, with special reference to the role of afferent inhibition in sensory perception and discrimination. Bull Johns Hopkins Hosp 105: 201–232
50. Nudo RJ, Jenkins WM, Merzenich MM (1990) Repetitive microstimulation alters the cortical representation of movements in adult rats. Somatosen Mot Res 7: 463–483
51. O'Leary DDM, Schlaggar BL, Tuttle R (1994) Specification of neocortical areas and thalamocortical connections. Annu Rev Neurosci 17: 419–439
52. Parnavelas JG, Stern CD, Stirling RV (1988) Sharpening the pattern. In: Parnavelas JG, Stern CD, Stirling RV (eds) The making of the nervous system. Part IV. Oxford University Press, Oxford
53. Pascual-Leone A, Torres F (1993) Plasticity of the sensorimotor cortex representation of the reading finger in Braille readers. Brain 116: 39–52
54. Pearson JC, Finkel LH, Edelman GM (1987) Plasticity in the organization of adult cerebral cortical maps: a computer simulation based on neuronal group selection. J Neurosci 7: 4209–4223
55. Poggio T, Fahle M, Edelman S (1992) Fast perceptual learning in visual hyperacuity. Science 256: 1018–1021
56. Pons TP, Garraghty PE, Mishkin M (1988) Lesion-induced plasticity in the second somatosensory cortex of adult macaques. Proc Natl Acad Sci USA 85: 5279–5281
57. Recanzone GH, Merzenich MM, Dinse HR (1992a) Expansion of the cortical representation of a specific skin field in primary somatosensory cortex by intracortical microstimulation. Cerebral Cortex 2: 181–196
58. Recanzone GH, Merzenich MM, Jenkins WM, Grajski K, Dinse HR (1992b) Topographic reorganization of the hand representation in cortical area 3b of owl monkeys trained in a frequency discrimination task. J Neurophysiol 67: 1031–1056
59. Recanzone GH, Merzenich MM, Schreiner CE (1992c) Changes in the distributed temporal response properties of SI cortical neurons reflect improvements in performance on a temporally-based tactile discrimination task. J Neurophysiol 67: 1071–1091
60. Recanzone GH, Schreiner CE, Merzenich MM (1993) Plasticity in the frequency representation of primary auditory cortex following discrimination training in adult owl monkeys. J Neurosci 13: 87–103
61. Ritter H, Martinetz T, Schulten K (1990) Neuronale Netze. Addison-Wesley, Reading, Mass
62. Robertson D, Irvine DRF (1989) Plasticity of frequency organization in auditory cortex of guinea pigs with partial unilateral deafness. J Comp Neurol 282: 456–471
63. Salzman CD, Britten KH, Newsome WT (1990) Cortical microstimulation influences perceptual judgements of motion direction. Nature 346: 174–177
64. Scheich H (1991) Auditory cortex: comparative aspects of maps and plasticity. Cur Opin Neurobiol 1: 236–247
65. Sholl DA (1956) The organization of the Cerebral Cortex. Methuen, London
66. Shuishi-Haupt S, Spengler F, Dinse HR (1994) A laminar analysis of cortical ICMS-induced representational plasticity. In: Elsner N, Breer H (eds) Sensory transduction. Thieme, Stuttgart
67. Sirois D, Hand P (1991) Microstimulation of rat "barrel" cortex results in an expanded metabolic and electrophysiologic cortical vibrissa representation. Soc Neurosci Abstr 17: 842
68. Sirosh J, Miikkulainen R (1994) Cooperative self-organization of afferent and lateral connections in cortical maps. Biol Cybern 71: 65–78
69. Spengler F (1993) Lernen und Vergessen in neuronalen Netzwerken. post-ontogenetische Plastizität. series 10, no. 271. VDI Verlag, Dusseldorf
70. Spengler F, Dinse HR (1994) Reversible relocation of representational boundaries of adult rats by intracortical microstimulation (ICMS). Neuroreport 5: 949–953
71. Spengler F, Godde B, Dinse HR (1995) Effects of aging on topographic organization of somatosensory cortex. Neuroreport 6: 469–473
72. Stoney SD, Thompson WD, Asanuma H (1968) Excitation of pyramidal tract cells by intracortical microstimulation: effective extent of stimulating current. J Neurophysiol 31: 659–669
73. Tommerdahl M, Favorov O, Whitsel BL, Nakhle B, Gonchar YA (1993) Minicolumnar activation patterns in cat and monkey SI cortex. Cerebral Cortex 3: 399–411
74. Weinberger NM, Ashe JH, Metherate R, McKenna TM, Diamond DM, Bakin J (1990) Retuning auditory cortex by learning: a preliminary model of receptive field plasticity. Concepts Neurosci 1: 91–132
75. Wilson HR, Cowan JD (1973) A mathematical theory of the functional dynamics of cortical and thalamic nervous tissue. Kybernetik 13: 55–80
76. Xerri C, Stern JM, Merzenich MM (1994) Alterations of the cortical representation of the rat ventrum induced by nursing behavior. J Neurosci 14: 1710–1721
77. Zepka RF, Spengler F, Dinse HR (1994) Fast and reversible reorganization of the thalamo-cortical pathway of adult rats induced by intracortical and intrathalamic microstimulation. Soc Neurosci Abstr 20: 1431